



Reagentless uric acid biosensor based on Ni microdiscs loaded NiO thin film matrix

Journal:	<i>Analyst</i>
Manuscript ID:	AN-ART-06-2014-001029.R1
Article Type:	Paper
Date Submitted by the Author:	25-Jun-2014
Complete List of Authors:	A, Kashima; University of Delhi, Physics and Astrophysics Tomar, Monika; Miranda House, University of Delhi, Department of Physics Gupta, Vinay; University of Delhi, Department of Physics and Astrophysics

1
2
3 ***Reagentless uric acid biosensor based on Ni microdiscs loaded NiO thin film matrix***
4

5 Kashima Arora¹, Monika Tomar² and Vinay Gupta^{*,1}
6

7 ¹*Department of Physics and Astrophysics, University of Delhi, Delhi 110007, India*
8

9 ²*Physics Department, Miranda House, University of Delhi, Delhi 110007, India*
10

11 *Corresponding Author's Email: vgupta@physics.du.ac.in
12

13 **Abstract**
14

15
16 Development of a non invasive test for uric acid has been the Holy Grail of uric acid detection
17 research for last decade. In the present work, a novel matrix comprising of NiO thin film (a
18 biocompatible material) loaded with Ni micro discs is prepared on ITO coated glass substrate
19 (Ni/NiO/ITO) with the help of RF sputtering technique for reagentless detection of uric acid. The
20 bioelectrode was fabricated by immobilizing Uricase using physical adsorption technique on the
21 surface of Ni/NiO/ITO electrode. The prepared matrix was found to be efficient in translating
22 biological processes, occurring on the surface of the bioelectrode (Ur/Ni/NiO/ITO) in the presence of
23 analyte (uric acid) to an electronic output. The biosensor exhibits a high sensitivity (431.09 $\mu\text{A}/\text{mM}$),
24 low value of K_m (0.15 mM), high apparent enzyme activity (5.07×10^{-2} units/cm²), high shelf life (20
25 weeks) and good selectivity for detection of uric acid over a wide concentration range (0.05 mM to 1
26 mM) without any external mediator in the PBS buffer. The obtained results are encouraging for the
27 realization of a reagentless uric acid biosensor with efficient sensing response characteristics.
28
29
30
31
32
33
34

35 **Keywords:** NiO, multi valence property, RF sputtering, thin film, uric acid biosensor.
36
37
38
39
40
41
42
43
44
45
46
47
48
49
50
51
52
53
54
55
56
57
58
59
60

Introduction

Uric acid is a product of the metabolic breakdown of purine nucleotides in the liver and is a chief nitrogenous component of biological fluids such as urine and blood serum. Estimation of uric acid concentration in blood has recently become clinically important for the diagnosis of various diseases such as gout, hyperuricemia or Lesch-Nyhan syndrome, arthritis, diabetes, renal, neurological, cardiovascular and kidney related problems.¹ Thus, precise detection of uric acid concentration level in blood is of significant interest for biomedical applications and requires immediate attention. A number of techniques have been used for detection of uric acid including amperometric, potentiometric, optical, thermal, piezoelectric etc.²⁻⁵ Amongst them, the enzyme(uricase) based amperometric biosensor is considered to be the most promising approach as it offers fast, simple and low-cost detection technique. Several matrices such as conducting polymers, CNTs, metal nanoparticles, composite thin films, etc. have been used to immobilize uricase for the fabrication of uric acid biosensors and are summarized in table 1.⁶⁻⁹ It may be noted from table 1 that most of the bioelectrodes exploited for detection of uric acid are found to suffer from certain problems such as lack of stability, time-consuming, non linear detection range, leaching out of immobilized enzyme, low sensitivity, and higher value of low detection limit and thereby limiting their application in development of an efficient uric acid biosensor. Recently, metal oxide based thin film matrix has gained significant attention for biosensing applications because of its biocompatibility, ease of processing, high stability, good sensitivity, excellent selectivity, low detection limit, low cost and capability of being fabricated in integrated biochip.¹⁰⁻¹³ Amongst various matrices, nickel oxide (NiO), a p-type and wide band gap (3.7 eV) semiconductor, is of immense interest. This matrix by its virtue of natural abundance, low cost, non-toxic, high chemical stability, biocompatibility, good electron communication feature and high isoelectric point (IEP ~ 10.7) is advantageous in binding biomolecules, which are having low IEP by strong electrostatic interaction. NiO thin films and their composites are efficiently used for the development of various biosensors for estimation of haemoglobin, glucose, metformin, uric acid etc.¹⁴⁻¹⁷ However, in all such estimations either sensitivity is poor or an external mediator in the PBS solution is used to get redox couple. Despite the fact that Ni has multivalence states (Ni^{2+} and Ni^{3+}), a novel approach is required to activate the electrocatalytic activity of the NiO based matrix. Since NiO has its own redox couple therefore it provides direct electron transfer between the redox protein and electrode, which thus may pave a way towards the realization of a reagentless bioelectrode for efficient detection of uric acid.

In this article a reagentless uric acid biosensor has been successfully fabricated using a novel matrix of NiO thin film matrix loaded with Ni microdiscs. The biosensing response characteristics of the prepared bioelectrode (Ur/Ni/NiO/ITO) as a function of uric acid concentration have been studied using amperometric and photometric techniques. The reagentless detection of uric acid with enhanced

sensing response has been obtained after integrating Ni microdiscs with NiO thin film using rf magnetron sputtering.

Experimental

Materials and methods

Uricase, horseradish peroxidase (HRP) (200Umg^{-1}), o-dianisidine were purchased from Sigma-Aldrich. Sodium phosphate monobasic anhydrous and sodium phosphate dibasic dihydrate were obtained from Sisco chemical, India. Deionized water (resistivity= $18.2\text{M}\Omega\text{ cm}^{-1}$) was used for the preparation of aqueous solutions.

Measurement and Apparatus

X-ray diffraction (XRD) for studying structural properties was carried out using Bruker X-ray diffractometer to identify the crystallographic structure of prepared matrices of NiO and Ni/NiO. The surface morphology of the film and bioelectrode was studied using scanning electron microscope (SEM). The photometric assay of the prepared bioelectrodes were performed using UV-visible spectrophotometer (Perkin Elmer:lambda 35) to investigate the binding of Uricase onto the electrode surface. Electrochemical measurements were conducted on Gamry potentiostat/galvanostat (Ref 600) using a three-electrodes cell containing Ag/AgCl as reference electrode, platinum (Pt) as counter electrode and the prepared electrodes (NiO/ITO and Ni/NiO/ITO) as the working electrode in PBS buffer of pH 7.0.

Preparation of Solutions

Phosphate buffer saline (PBS) (50mM, pH 7.0) solution was prepared by adjusting the proportion of monobasic sodium phosphate and dibasic sodium phosphate solutions and then adding 0.9%NaCl to the solution. Uricase (1mgmL^{-1}) and HRP solutions (1mgmL^{-1}) were freshly prepared in PBS buffer (pH 7.0). Different concentrations of uric acid solution (0.05 – 1.00 mM) and solution of o-dianisidine (1%) dye were freshly prepared in de-ionized water.

Preparation of NiO thin film and Ni microdiscs/NiO thin film matrices and immobilization of uricase

NiO film of thickness 245 nm was deposited on ITO coated Corning glass substrate (ITO/glass) using rf-magnetron sputtering technique. A nickel metal target (99.99% pure and 2 inch diameter) was sputtered in a reactive gas mixture (50% O₂ and 50% Ar) at a growth pressure of 30 mT using 40W rf power without any external substrate heating. ITO coated corning glass substrates of area 2.0 cm×0.5 cm was used, out of which 1.0 cm×0.5 cm of area was masked for the electrical contacts and the NiO

1
2
3 thin film was deposited on remaining area of 1.0 cm×0.5 cm area of ITO/glass substrate. A schematic
4 of the sensor structure prepared in the present study is shown in fig.1. Microdiscs of Ni of 100 nm
5 thickness were deposited onto the surface of NiO thin film (Ni/NiO/ITO) using rf sputtering through a
6 shadow mask (pore diameter ~ 250 μm), in an ambient of Ni of 100 % Ar, at a growth pressure of 10
7 mT and by applying an RF power of 40 W. The electrode without Ni microdiscs (NiO/ITO) was also
8 prepared for comparison with Ni/NiO/ITO electrode (Fig.1). Uricase (Ur) enzyme was immobilized
9 on the surface of both the electrodes (NiO/ITO and Ni/NiO/ITO) by physical adsorption technique.
10 The 0.5 cm² area of both the electrodes were dipped in a solution of Uricase (1mg/ml) that was
11 prepared in 50 mM (0.9% NaCl) phosphate buffer saline (PBS). The electrodes were kept overnight
12 for enzyme (Uricase) immobilization and subsequently washed with PBS solution and dried under
13 nitrogen flow. The schematic of immobilization of uricase on the surface of Ni/NiO/ITO matrix is
14 shown in figure 2. The prepared bioelectrodes Ur/Ni/NiO/ITO and Ur/NiO/ITO (fig.1) were stored at
15 4 °C when not in use.
16
17
18
19
20
21
22
23

24 **Results and Discussion**

25
26 NiO/ITO and Ni microdiscs/NiO/ITO matrices deposited by RF sputtering under the optimized
27 growth conditions were found to be smooth, and strongly adherent to all the substrates.
28
29

30 **Structural property**

31
32 As-deposited NiO thin film deposited at room temperature was found to be amorphous and becomes
33 polycrystalline when annealed in air at a temperature of 100 °C for one hour in air. XRD spectra of
34 the NiO and Ni/NiO matrices deposited on ITO coated corning glass substrate after post deposition
35 annealing at 100°C are shown in the inset of Figure 3. The XRD spectra of NiO thin films exhibits
36 three well defined diffraction peaks corresponding to (111), (200) and (220) planes of NiO thus
37 indicating growth of polycrystalline thin film (inset of Fig.3). Additional peak observed at 2θ ~51.6°
38 in the XRD pattern of Ni/NiO matrix corresponds to the Ni and confirms the presence of Ni
39 microdiscs on the surface of NiO thin film matrix.¹⁸
40
41
42
43
44

45 **Optical property**

46
47 NiO and Ni/NiO matrix were also deposited on corning glass substrate (without ITO coating) under
48 similar deposition conditions for optical characterization. UV-Visible transmission spectra of NiO and
49 Ni/NiO recorded over the wavelength range 190 to 1100 nm is shown in Fig.3. The NiO thin film was
50 found to exhibit a value of relatively low transmission (~65 %) in the visible region (Fig.3), indicating
51 the growth of metal rich NiO thin film under oxygen deficient reactive gas environment. It may be
52 noted from Fig.3 that the optical transmission further decreases to about 50% in the visible region
53 when Ni microdiscs are integrated with NiO thin film. Both thin film matrices showed a sharp fall in
54
55
56
57
58
59
60

1
2
3 the UV region at around 310 nm corresponding to the onset of fundamental absorption edge (Fig.3).
4 The band gap of NiO and Ni/NiO thin film matrices was evaluated using Tauc plots and its value was
5 found to be about 3.78 to 3.53 eV respectively. The value of 3.78 is in agreement with the
6 corresponding value reported for NiO thin film by other workers.¹⁹ However, the value of E_g is
7 slightly reduced to 3.53 eV after integrating with Ni microdiscs.
8
9

10 11 **Surface Morphology**

12
13 The surface morphologies of (i) NiO/ITO electrode and (ii) Uricase/NiO/ITO bioelectrode were
14 studied using SEM and images are shown in figure 4 (i) and (ii) respectively. The surface of NiO thin
15 film shows a fine homogeneous morphology having uniformly distributed nanosize crystallites [fig.4
16 (i)]. The surface morphology becomes rough after immobilization of macro molecules of Uricase
17 enzyme (1 mg/ml) onto the surface of NiO/ITO electrode. The uniformly distributed globular
18 structure observed in the SEM image of the surface of Uricase/NiO/ITO biosensor [Figure 4 (ii)]
19 reveals successful binding of enzyme with homogeneous coverage as well as dense loading.
20
21
22
23

24 25 **Electrochemical property**

26 27 **NiO/ITO electrode:**

28
29 In our earlier work, fabrication of a NiO thin film based uric acid biosensor was reported where
30 sensing was carried out in a mediated buffer.¹ For the development of reagentless NiO based
31 biosensor, deposition conditions of NiO thin films were varied so that the redox properties of NiO
32 matrix could be obtained without using any external mediator in the buffer solution.
33
34
35

36
37 CV response of the NiO/ITO electrode thin film in a reagentless PBS buffer in the potential range -0.3
38 to 0.8 V is shown in Figure 5(a). It may be noted from Fig.5(a) that well defined oxidation and
39 reduction peaks are obtained for the Ni^{3+}/Ni^{2+} redox couple in the NiO thin film matrix. It is important
40 to point out the CV curves obtained for the electrodes having NiO thin films of different thickness
41 (180 nm to 270 nm), that are shown in Figure 5(a). With increasing the thickness of NiO thin film
42 from 180 to 245 nm, peak oxidation current increases continuously from 27 μA to 50 μA and
43 decreases thereafter with further increasing the thickness (> 245 nm) of NiO thin film. Therefore,
44 245nm thin NiO film is used for the preparation of bioelectrodes for further study.
45
46
47
48

49
50 CV curve, obtained after immobilizing Uricase on the surface of NiO/ITO electrode, reflects a
51 decrease in the peak oxidation current from 50 μA to 23 μA . The decrease is due to the non-
52 conducting nature of the macromolecules of Uricase.
53
54

55
56 Figure 5(c) shows the amperometric sensing response of Ur/NiO/ITO bioelectrode on successive
57 addition of uric acid in the PBS solution. It may be seen that the peak oxidation current of the
58
59
60

bioelectrode increases linearly from 35 μA to 169 μA with respect to increase in the uric acid concentration from 0.05 to 1.00 mM (Fig.5 (d)) with a correlation coefficient (R) of 0.98, indicating good electrocatalytic behaviour of the NiO matrix. The sensitivity of the Ur/NiO/ITO bioelectrode as calculated from the calibration curve is found to be about 76.41 $\mu\text{A}/\text{mM}$. The obtained results are slightly inferior to the corresponding one reported by other workers who have reported on uric acid biosensors using external mediators,²⁰ however, the reagentless detection in the present study is advantageous.

Ni/NiO/ITO electrode:

The CV response of the Ni/NiO/ITO electrode, having Ni microdiscs, were studied in a PBS buffer without any mediator. The corresponding curve obtained for bare NiO/ITO electrode (without Ni microdiscs) is also included in Fig.6 (a) for comparison. A drastic enhancement in the peak oxidation current from 50 μA to 250 μA was observed as a result of the integration of Ni microdiscs with the surface of NiO/ITO electrode (Fig. 6 (a)). The presence of Ni microdiscs provided excess charge carriers for the transport via $\text{Ni}^{3+}/\text{Ni}^{2+}$ redox couple for obtaining a CV curve that showed enhanced oxidation peak current obtained without any mediator in the buffer. A decrease in the peak oxidation current from 250 μA to 152 μA was observed when uricase was immobilized on the surface of Ni/NiO/ITO electrode (Fig.6 (b)) and was attributed to the non-conducting nature of the macromolecules of uricase.

Amperometric sensing response Characteristics: Ur/Ni/NiO/ITO bioelectrode as a function of uric acid:

Concentration is shown in Fig.6 (c) in a reagent free PBS solution. A linear increase in the peak oxidation current from 283 μA to 655.33 μA was observed for the Ur/Ni/NiO/ITO bioelectrode, affected by the increase in the concentration of uric acid from 0.05 to 1.0 mM. The sensitivity of the bioelectrode (Ur/Ni/NiO/ITO) having Ni microdiscs, was found to be about 431.09 $\mu\text{A}/\text{mM}$ (fig. 6(d)) which is much higher compared to the corresponding value (76.41 $\mu\text{A}/\text{mM}$) obtained for uricase/NiO/ITO bioelectrode. The detection limit is found to be about 0.06 mM. The lower detection limit is calculated using the expression $3S_{y/x}/\text{sensitivity}$, where $S_{y/x}$ is standard deviation obtained from the peak oxidation current vs analyte concentration curve (figure 6 (d)). The obtained value of sensitivity for Ni microdiscs based bioelectrode was found to be much higher in comparison to the corresponding value reported for uric acid biosensors by various workers in the literature [table 1], and is attributed to the availability of both Ni microdiscs and uncovered surface of NiO thin film that resulted the immobilization of uricase and subsequently faster transfer of large amount of charge carriers from enzyme to electrode.

Michaelis Menten Kinetic parameter (K_m)

The graph between the ratio of analyte concentration to the oxidation peak current and the analyte concentration (Hanes plot) was plotted and utilized to evaluate the value of Michaelis-Menten constant (K_m) for both uricase/NiO/ITO and uricase/Ni/NiO/ITO bioelectrodes, and is found to be about 0.21 and 0.15 mM respectively. The low value of K_m (0.15 mM) obtained for uricase/Ni/NiO/ITO bioelectrode indicates the high affinity of the immobilized uricase towards its analyte (uric acid) and is attributed to the effective loading of enzyme due to high surface area along with high electron communication property of the prepared matrix having NiO thin film loaded with Ni microdiscs. The bioelectrode having Ni microdiscs (Ur/Ni/NiO/ITO) was also found to attain about 98% of its steady state in less than 5 sec, indicating the fast electron communication between the immobilized uricase and the electrode via Ni/NiO matrix.

Photometric enzyme assay

To carry out the photometric enzyme assay, both the bioelectrodes were dipped separately in 3 ml PBS solution containing 20 μ l horseradish peroxidase (HRP), 20 μ l *o*-dianisidine dye and 100 μ l of analyte (uric acid) in varying concentration. The difference between the initial and final values of absorbance value at $\lambda = 500$ nm were recorded after 2 min. of analyte and are shown in Fig. 6 (e) as a function of the concentration of uric acid. The uricase enzyme activity increases with an increase in the concentration of uric acid upto 0.5 mM for both the bioelectrodes and thereafter shows a saturating tendency with further increase in concentration (> 0.5 mM). The amount of bound enzyme is determined from the apparent enzyme activity (α_{enz}^{app}) calculated using equation

$$\alpha_{enz}^{app} (\text{Ucm}^{-2}) = \frac{AV}{\epsilon ts} \quad (1)$$

where A is the difference in absorbance of bioelectrode before and after incubation, V is the total volume ($= 3.17 \text{ cm}^3$), ϵ is the millimolar extinction coefficient for *o*-dianisidine ($\epsilon \sim 7.5$ for at 500 nm), t is the reaction time (2 min), and s is the surface area of the electrode ($1.0 \times 0.5 \text{ cm}^2$). The values of apparent enzyme activity of uricase immobilized on the surface of NiO/ITO and Ni/NiO/ITO electrodes are found to be about $4.14 \times 10^{-2} \text{ unit/cm}^2$ and $5.07 \times 10^{-2} \text{ unit/cm}^2$ respectively. The obtained results clearly indicate that the composite matrix of NiO thin film loaded with Ni microdiscs provides a better platform for effective and conformal immobilization of enzyme and hence more units of uricase are actively working on its unit surface area. The obtained results in present work are found to be better in comparison to those reported in literature by other workers for uric acid biosensors but without any external mediator in the PBS solution, and is attributed to the integration of Ni microdiscs with NiO matrix [Table 1].

Real sample analysis

As we know, for thorough evaluation of the analytical performance of the proposed method the limit of detection, linearity, precision, stability, accuracy and selectivity have to be fulfilled by the prepared uricase/Ni/NiO/ITO/glass biosensor. Therefore, to demonstrate the practical feasibility of prepared uricase/Ni/NiO/ITO/glass biosensor for the analysis of uric acid in the real biological fluid, 10 human sera samples were analyzed and the % recovery and precision were calculated for spiked samples. After the addition of the sera samples in the electrolyte solution, the peak oxidation current values were noted from the CV measurements. Uric acid concentration in serum was then extrapolated from the standard calibration curve, plotted between uric acid concentration (mM) and current (figure 6 (d)). Electrochemical sensing technique in the present work was used to corroborate results obtained from commercial spectrophotometric method in the clinical laboratory. To validate the accuracy, the content of uric acid in serum samples determined by the prepared biosensor was compared with that measured by commercial spectrophotometric method in the clinical laboratory. Table 2 summarizes the results obtained during the present investigation. The results indicate that the uric acid analysis in sera with the developed biosensor agrees well with the spectrophotometric data. Recovery tests were also performed, in order to demonstrate the accuracy and precision of the prepared biosensor, by adding a known concentration of uric acid (0.50 mM) in the already tested serum samples and then estimating the concentration of added uric acid (Table 2). The performed recovery tests confirm that the fabricated biosensor is accurate and precise. The performance of the prepared biosensor system is comparable with the commercially accepted methods. For in-vivo application of the biosensor in clinical practice, the requirements of biocompatibility, linearity, sensitivity, specificity, accuracy and long-term stability were very well fulfilled by uricase/Ni/NiO/ITO based biosensor.

Conclusion

In summary an efficient and reagentless uric acid biosensor is developed using a novel matrix of NiO thin film loaded with Ni microdiscs. Ni microdiscs distributed uniformly on the surface of NiO/ITO electrode, provides an attractive platform for effective immobilization of uricase, by using physical adsorption technique. The activation of $\text{Ni}^{2+}/\text{Ni}^{3+}$ redox couple in the matrix helps in realization of a reagentless detection of uric acid as well as enhanced sensing response. The prepared uricase/Ni/NiO/ITO bioelectrode exhibits high sensitivity (431.09 $\mu\text{A}/\text{mM}$), good linearity over a wide range of uric acid concentration (0.05 to 1.00 mM), low value of K_m (0.15 mM) and a low detection limit (0.03 mM). The results obtained using novel matrix of Ni microdiscs loaded NiO thin films are encouraging for the realization of an efficient uric acid biosensor.

Acknowledgement

1
2
3 Authors are thankful to Department of Science and Technology (DST) and UGC for the financial
4 support to carry out the proposed work. One of the authors (KA) acknowledges CSIR for fellowship.
5
6

7 **Figure Captions:**
8

9 Figure 1. Schematic of the prepared Ur/NiO/ITO and Ur/Ni/NiO/ITO bioelectrodes.
10

11 Figure 2. Schematic and flowchart of the preparation of Ur/Ni/NiO/ITO bioelectrode using
12 immobilized uricase via physical adsorption technique.
13

14 Figure 3. UV-Visible transmission spectra of NiO/glass and Ni/NiO/glass substrates; Inset shows the
15 X-ray diffraction of NiO/glass and Ni/NiO/glass structure.
16

17 Figure 4. SEM image of (a) NiO/ITO matrix and (b) Uricase immobilized on NiO/ITO.
18

19 Figure 5. (a) Cyclic Voltammogram of NiO/ITO electrode having different thickness of NiO film; (b)
20 shows the variation of peak oxidation current with thickness, (c) Amperometric sensing response of
21 Ur/NiO/ITO bioelectrode with an increase in uric acid concentration; (d) shows Variation of peak
22 oxidation current with uric acid concentration.
23

24 Figure 6. (a) Cyclic Voltammogram (CV) of Ni/NiO/ITO and NiO/ITO electrodes; (b) shows CV of
25 Ni/NiO/ITO electrode and Ur/Ni/NiO/ITO bioelectrode, (c) Sensing response of uricase/Ni/NiO/ITO
26 bioelectrode as a function of the uric acid concentration: (i) 0.05 (ii) 0.1 (iii) 0.2 (iv) 0.3 (v) 0.4 (vi)
27 0.5 (vii) 0.7 and (viii) 1.00 mM, (d) shows the variation of peak oxidation current as a function of
28 concentration of uric acid and (e) shows the photometric assay of uricase/Ni/NiO/ITO and
29 uricase/NiO/ITO bio-electrodes as a function of uric acid concentration.
30
31

32 **Table Captions:**
33

34 Table 1. Brief summary of the amperometric sensing parameters of uric acid biosensors reported
35 by various workers. The corresponding Ni/NiO/ITO electrode is also included for comparison.
36

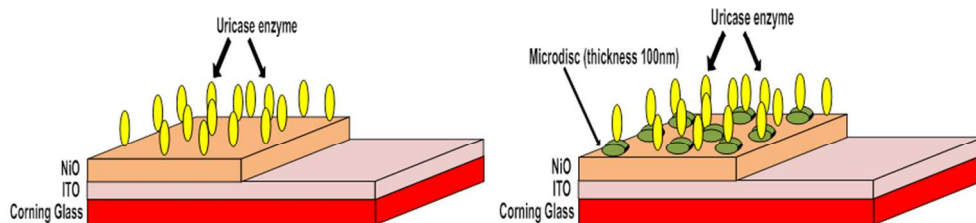
37 Table 2. Determination and recovery of uric acid in human serum samples using the prepared
38 Uricase/Ni/NiO/ITO/glass biosensor.
39
40
41
42
43
44
45
46
47
48
49
50
51
52
53
54
55
56
57
58
59
60

References

- 1 K. Arora, M. Tomar, and V. Gupta, *Biosens. Bioelectron.* 30 (2011) 333.
- 2 P. Schrenkhammer, and O. S. Wolfbeis, *Biosens. and Bioelectron.* 24 (2008) 994.
- 3 T. M. Pan, K. Y. Chang, C. W. Lin, S. W. Tsai, and M. H. Wu, *Sensors and Actuators B* 160 (2011) 850.
- 4 R. Konck, T. Lenarczuk, A. Radomska, and S. Glab, *Analyst* 126 (2001) 1080.
- 5 Z. Yang, S. Si, H. Dai, and C. Zhang, *Biosens. Bioelectron.* 22 (2007) 3283.
- 6 T. Ahuja, Rajesh, D. Kumar, V. K. Tanwar, V. Sharma, N. Singh, and A. M. Biradar, *Thin Solid Films* 519 (2010) 1128.
- 7 S. M. U. Ali, N. H. Alvia, Z. Ibupoto, O. Nur, M. Willander, and B. Danielsson, *Sensors and Actuators B* 152 (2011) 241.
- 8 X. Wang, T. Hagiwara, and S. Uchiyama, *Anal. Chim. Acta* 587 (2007) 41.
- 9 K. Arora , G. Sumanaa, V. Saxena, R. K. Gupta, S. K. Gupta, J. V. Yakhmi, M. K. Pandey, S. Chand, and B.D. Malhotra, *Anal. Chim. Acta* 594 (2007) 17.
- 10 F. Zhang, X. Wang, S. Ai, Z. Sun, Q. Wan, Z. Zhu, Y. Xian, L. Jin, and K. Yamamoto, *Anal. Chim. Acta* 519 (2004) 155.
- 11 S. P. Singh, S. K. Arya, P. Pandey, B. D. Malhotra, S. Saha, K. Sreenivas, and V. Gupta, *Appl. Phys. Lett.*, 91 (2007) 063901.
- 12 S. Saha, S. K. Arya, S. P. Singh, K. Sreenivas, B. D. Malhotra, and V. Gupta, *Anal. Chim. Acta*, 653 (2009) 212.
- 13 S. Saha, and V. Gupta,. *J. Appl. Phys.*, 110 (2011) 064904.
- 14 A. Salimi, E. Sharifi, A. Noorbakhsh, and S. Soltanian, *Biophys. Chem.* 540 (2007) 125.
- 15 W. D. Zang, C. Jin, J. L. Chuan, Y. Y. Xiang, Z. J. Qi, *Mikrochim. Acta* 168 (2010) 259.
- 16 A. Safavi, N. Maleki, and E. Farjami, *Biosens. Bioelectron.* 24 (2009) 1655.
- 17 N. Sattarahmady, H. Heli, F. Faramarzi, *Talanta* 82 (2010) 1126.
- 18 H. Sato, T. Minami, S. Takata, and T. Yamada, *Thin Solid Films* 236 (1993) 27.
- 19 M. Tyagi, M. Tomar, and V. Gupta, *Anal. Chim. Acta* 726 (2012) 93.
- 20 Y. Liu, M. Yuan, L. Liu, and R. Guo, *Sensors and Actuators B* 176 (2013) 592.
- 21 Y. Wang, and Y. Hasebe, *Pharmaceutical and Biomedical Analysis* 57 (2012) 125.

- 1
2
3 22 X. Liu, Y. Peng , X. Qua, S. Ai, R. Han, and X. Zhu, *Electroanal. Chem.* 654 (2011) 72.
4
5 23 J. M. Zen, Y. Y. Lai, H. H. Yang, and A. S. Kumar, *Sens. and Actuators B* 84 (2002) 237.
6
7 24 E. Miland, and A.J. Miranda, *Talanta* 43 (1996) 785.
8
9 25 M. Hadi, and A. Rouhollahi, *Anal. Chim. Acta* 721 (2012) 55.
10
11 26 Z. H. Sheng, X. Q. Zheng, J. Y. Xua, W. J. Bao, F. B. Wang, and X. H. Xia, *Biosens. Bioelectron.*
12 34 (2012) 125.
13
14 27 R. M. A. Tehrani, and S. A. Ghani, *Sensors and Actuators B* 145 (2010) 20.
15
16 28 S. Prakash, T. Chakrabarty, A. M. Rajesh, and V. K. Shahi, *Measurement* 45 (2012) 500.
17
18 29 N. Chauhan, and C. S. Pundir, *Analytical Biochemistry* 413 (2011) 97.
19
20 30 S. B. Revin, and S. A. John, *Bioelectrochemistry* 88 (2012) 22.
21
22 31 H. Chu, X. Wei, M. Wu, J. Yan, and Y. Tu, *Sensors and Actuators B* 163 (2012) 247.
23
24 32 J. Arora, S. Nandwani, M. Bhambi, and C. S. Pundir, *Anal. Chim. Acta*, 647 (2009) 195.
25
26 33 P. Y. Chen, R. Vittal, P. C. Nien, G. S. Liou, and K. C. Ho *Talanta* 80 (2010) 1145.
27
28 34 Y. C. Luo, J. S. Do, and C. C. Liu, *Biosens. Bioelectron.* 22 (2006) 482.
29
30 35 D. M. Perez, M. L. Ferrer, and C. R. Mateo, *Anal. Biochem.* 322 (2003) 238.
31
32 36 R. Rawal, S. Chawla, N. Chauhan, T. Dahiya, and C.S. Pundir, *International Journal of Biological*
33 *Macromolecules* 50 (2012) 112.
34
35 37 S. Behera, and C. R. Raj, *Biosens. Bioelectron.* 23 (2007) 556.
36
37
38
39
40
41
42
43
44
45
46
47
48
49
50
51
52
53
54
55
56
57
58
59
60

1
2
3
4
5
6
7
8
9
10
11
12
13
14
15
16
17
18
19
20
21
22
23
24
25
26
27
28
29
30
31
32
33
34
35
36
37
38
39
40
41
42
43
44
45
46
47
48
49
50
51
52
53
54
55
56
57
58
59
60



254x190mm (96 x 96 DPI)

1
2
3
4
5
6
7
8
9
10
11
12
13
14
15
16
17
18
19
20
21
22
23
24
25
26
27
28
29
30
31
32
33
34
35
36
37
38
39
40
41
42
43
44
45
46
47
48
49
50
51
52
53
54
55
56
57
58
59
60

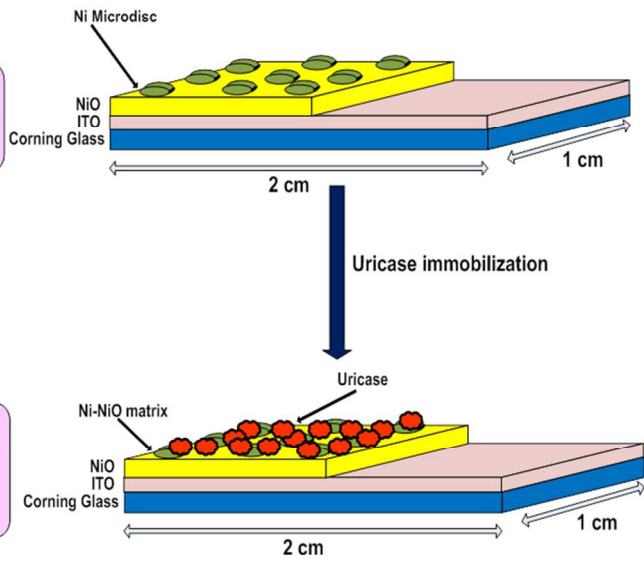
FLOWCHART

Ni microdisc loaded on NiO thin films deposited on ITO coated corning glass.

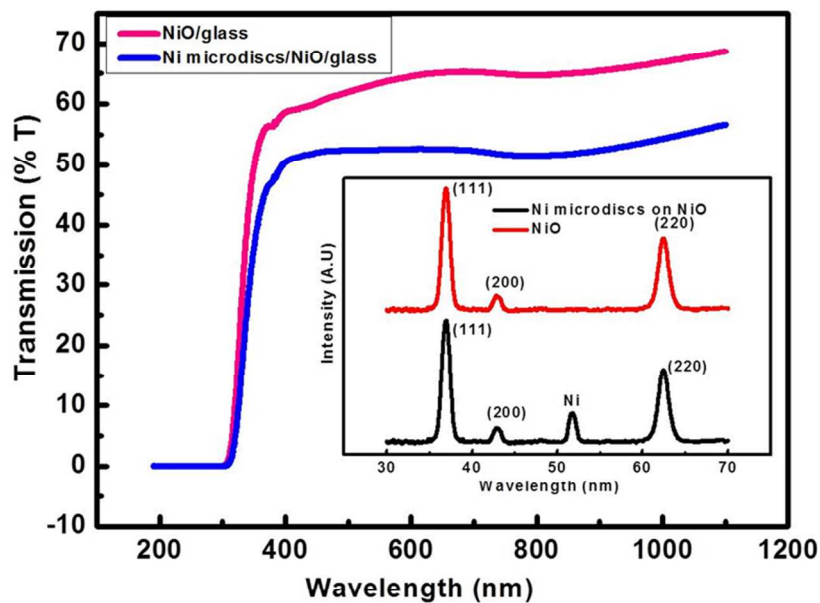


Immobilization of uricase on Ni-NiO matrices via physical adsorption

SCHEMATIC



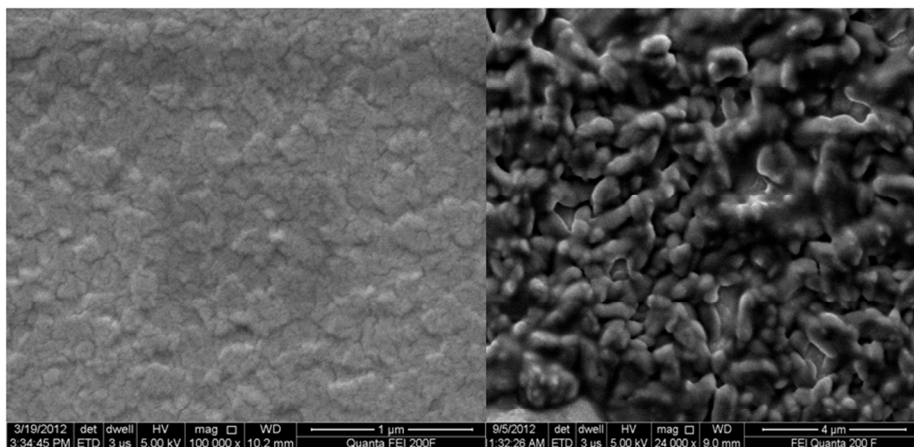
254x190mm (96 x 96 DPI)



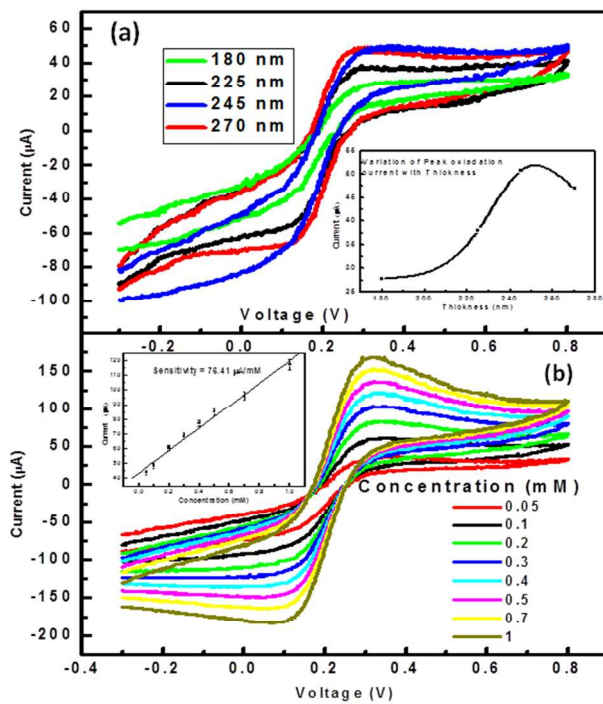
254x190mm (96 x 96 DPI)

1
2
3
4
5
6
7
8
9
10
11
12
13
14
15
16
17
18
19
20
21
22
23
24
25
26
27
28
29
30
31
32
33
34
35
36
37
38
39
40
41
42
43
44
45
46
47
48
49
50
51
52
53
54
55
56
57
58
59
60

1
2
3
4
5
6
7
8
9
10
11
12
13
14
15
16
17
18
19
20
21
22
23
24
25
26
27
28
29
30
31
32
33
34
35
36
37
38
39
40
41
42
43
44
45
46
47
48
49
50
51
52
53
54
55
56
57
58
59
60

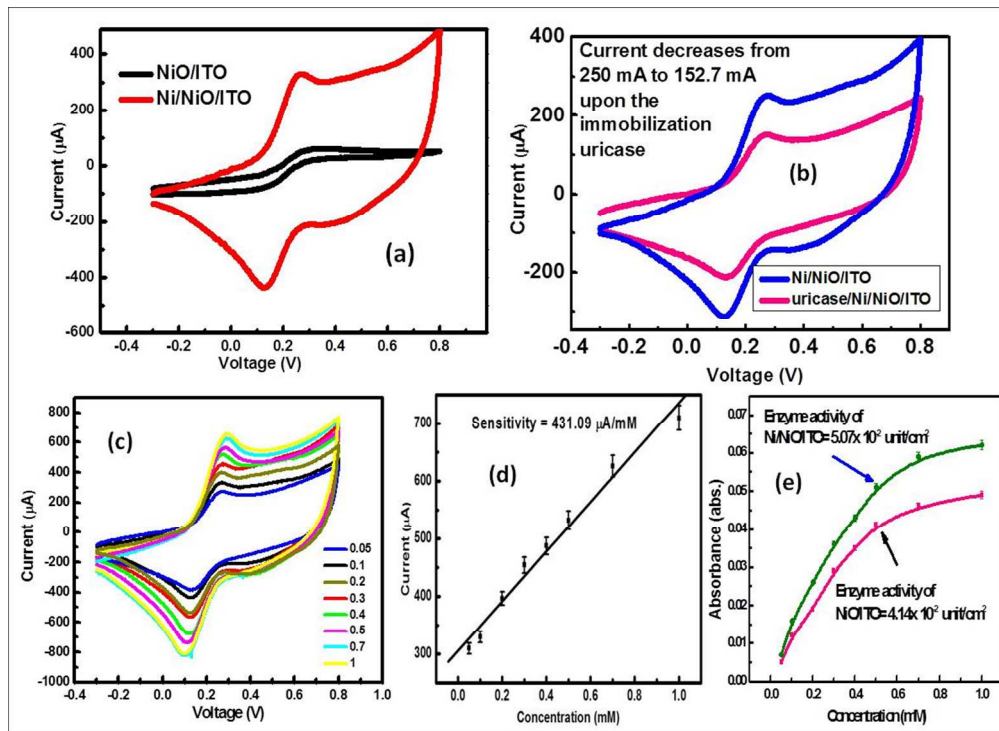


254x190mm (96 x 96 DPI)



254x190mm (96 x 96 DPI)

1
2
3
4
5
6
7
8
9
10
11
12
13
14
15
16
17
18
19
20
21
22
23
24
25
26
27
28
29
30
31
32
33
34
35
36
37
38
39
40
41
42
43
44
45
46
47
48
49
50
51
52
53
54
55
56
57
58
59
60



251x182mm (120 x 120 DPI)

1
2
3
4
5
6
7
8
9
10
11
12
13
14
15
16
17
18
19
20
21
22
23
24
25
26
27
28
29
30
31
32
33
34
35
36
37
38
39
40
41
42
43
44
45
46
47
48
49
50
51
52
53
54
55
56
57
58
59
60

S.No.	Material	Range (mM)	Sensitivity ($\mu\text{A mM}^{-1}$)	Response time (sec.)	Detection limit (mM)	S/N	Reference
1.	SAM of APTES Bisulfosuccinimide/ITO	0.05-0.58	39.35	50	0.037	3	6
2.	Gold electrode/polystyrene	$(5 \times 10^{-3} - 105 \times 10^{-3})$		60			8
3.	Carbon felt based H_2O_2	$(0.3 \times 10^{-3} - 20 \times 10^{-3})$	0.25		0.18×10^{-3}	3	21
4.	MWCNT-Ch/poly(amidamine)/DNA/gold electrode	$(0.5 \times 10^{-3} - 100 \times 10^{-3})$	43.9×10^{-6}	5s	0.07×10^{-3}	3	22
5.	Polyaniline	0.01-0.6	47.2	60s	0.01		9
6.	Polyurethane hydrogel	0-2		80-100s			2
7.	Screen printed electrode	$2 \times 10^{-3} - 40 \times 10^{-3}$	3.05		0.42×10^{-3}		23
8.	Poly(o-aminophenol) C paste electrode	0.1	5	37	3×10^{-3}		24
9.	Pyrolytic C film electrode		61.92		0.03×10^{-3}		25
10.	N doped graphene	$1 \times 10^{-4} - 2 \times 10^{-2}$			4.5×10^{-5}	3	26
11.	Zn-Ni nanoalloy/graphite	$1 \times 10^{-3} - 400 \times 10^{-3}$			0.2×10^{-3}	3	27
12.	Polyelectrolyte PDDA	$1 \times 10^{-3} - 60 \times 10^{-3}$	50		1×10^{-3}		28
13.	MWCNT/Au nps.	0.01-0.8	44	7	0.01	3	29

1
2
3
4
5
6
7
8
9
10
11
12
13
14
15
16
17
18
19
20
21
22
23
24
25
26
27
28
29
30
31
32
33
34
35
36
37
38
39
40
41
42
43
44
45
46
47
48
49
50
51
52
53
54
55
56
57
58
59
60

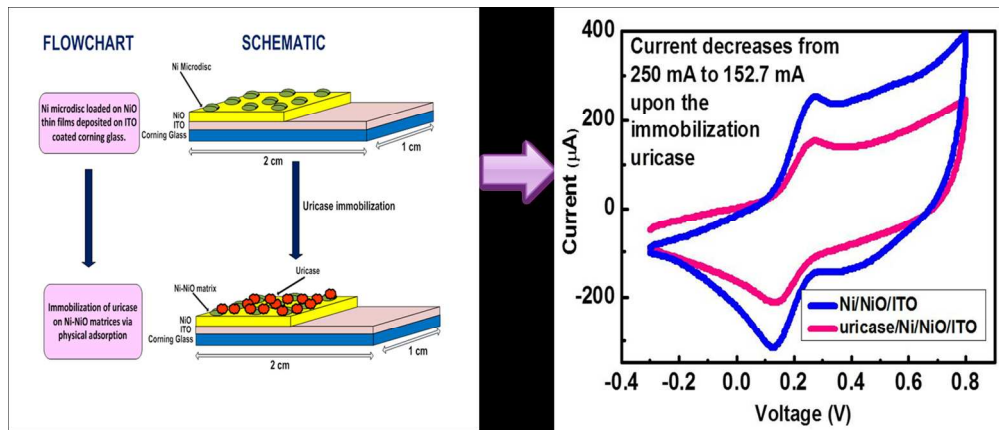
14.	3 amino5-mercapto-124 triazole/GC	40×10^{-6} - 0.1		50	0.52×10^{-6}	3	30
15.	polypyrrole/Pt	7.5×10^{-8} – 8.3×10^{-3}			75×10^{-9}		31
16.	Epoxy resin biocomposite	0.025-0.1		12	4.25	3	32
17.	Mol.Imprinted polymer (MIP)	0-1.125	24.72		0.3×10^{-3}	3	33
18.	Ir-C electrode	0.1-0.8	16.60	<45	0.01	6.18	34
19.	Ur-Peroxidase + Amplex red	1×10^{-3}			20×10^{-6}		35
20.	PB nps/MWCNT/P ANI/Au composite	0.005-0.8		4	5×10^{-3}	3	36
21.	SAM thio-substituted nucleobases/Au	1×10^{-3} - 500×10^{-3}	0.78	8	1×10^{-3}		37
	Ni micro discs/NiO/ITO matrix	0.05 – 1	431.09	4	0.03	3	Present work

1
2
3
4
5
6
7
8
9
10
11
12
13
14
15
16
17
18
19
20
21
22
23
24
25
26
27
28
29
30
31
32
33
34
35
36
37
38
39
40
41
42
43
44
45
46
47
48
49
50
51
52
53
54
55
56
57
58
59
60

Real Sample (Serum)	Concentration of uric acid measured (mM)		R.S.D. of developed biosensor (n=5) (%)	Spike (mM)	Concentration of uric acid detected (mM)	Recovery (%)	R.S.D. of developed biosensor (n=5) (%)
	Uricase/Ni/NiO/ITO/glass biosensor	Spectrophotometric method					
1	0.315	0.319	1.5	0.5	0.831	103.2	1.2
2	0.238	0.243	1.2	0.5	0.751	102.6	1.4
3	0.667	0.676	2.3	0.5	1.180	102.6	2.7
4	0.483	0.489	2.5	0.5	0.99	101.4	1.9
5	0.107	0.112	1.7	0.5	0.601	98.8	2.0
6	0.558	0.552	1.3	0.5	1.101	108.6	1.5
7	0.295	0.292	3.1	0.5	0.78	97	2.5
8	0.713	0.717	2.1	0.5	1.214	100.2	1.9
9	0.887	0.883	1.8	0.5	1.39	100.6	2.0
10	0.612	0.608	1.6	0.5	1.11	99.6	1.3

249x130mm (120 x 120 DPI)

1
2
3
4
5
6
7
8
9
10
11
12
13
14
15
16
17
18
19
20
21
22
23
24
25
26
27
28
29
30
31
32
33
34
35
36
37
38
39
40
41
42
43
44
45
46
47
48
49
50
51
52
53
54
55
56
57
58
59
60



253x108mm (150 x 150 DPI)